Many-body effects on nonadiabatic Feshbach conversion in bosonic systems

Jie Liu,[1,2] Bin Liu,[3,4] and Li-Bin Fu[2]
[1]*Center for Applied Physics and Technology, Peking University, Beijing 100084, People's Republic of China*
[2]*Institute of Applied Physics and Computational Mathematics, Beijing 100088, People's Republic of China*
[3]*Graduate School, China Academy of Engineering Physics, Beijing 100088, People's Republic of China*
[4]*College of Physics and Information Engineering, Hebei Normal University, 050016 Shijiazhuang, China*
(Received 2 January 2008; published 16 July 2008)

We investigate the dynamics of converting cold bosonic atoms to molecules when an external magnetic field is swept across a Feshbach resonance. Our analysis relies on a quantum microscopic model that accounts for many-body effects in the association process. We show that the picture of two-body molecular production depicted by the Landau-Zener model is significantly altered due to many-body effects. In the nonadiabatic regime, we derive an analytic expression for molecular conversion efficiency that explains the discrepancy between the prediction of the Landau-Zener formula and the experimental data [E. Hodby *et al.*, Phys. Rev. Lett. **94**, 120402 (2005)]. Our theory is further extended to the formation of heteronuclear diatomic molecules and gives some interesting predictions.

DOI: 10.1103/PhysRevA.78.013618 PACS number(s): 03.75.Mn, 03.75.Hh, 67.60.Bc

I. INTRODUCTION

The production of ultracold diatomic molecules is an exciting area of research with important applications ranging from the search for the permanent electric dipole moment [1] to BCS-BEC (Bose-Einstein condensate) crossover physics [2]. A widely used production technique involves the association of ultracold atoms into very weakly bound diatomic molecules by applying a time varying magnetic field in the vicinity of a Feshbach resonance [3,4]. The underlying conversion dynamics is usually described by the Landau-Zener (LZ) model [5]. In this model, the Feshbach molecular production is discussed under a two-body configuration where a single pair of atoms is converted to a molecule at an avoided crossing between atomic energy level and molecular energy level while the molecular energy is lifted by an applied linearly sweeping magnetic field. Thus, the molecular production efficiency is expected to be an exponential Landau-Zener type [6,7]. However, recent experimental data on ^{85}Rb by the JILA group showed a large discrepancy from the Landau-Zener formula: The value of the LZ parameter extracted from the data is 8 times larger than the prediction of LZ theory [8]. The experiment was performed under unusually low densities of the atom cloud ($\sim 10^{11}$ cm^{-3}) and the data were measured in the nonadiabatic regime so that the inverse ramp rate was less than 100 μs/G. Therefore, two- and three-body atomic decay and collisional molecular decay rates are negligible and do not affect the measurement. This puzzle remains unresolved and challenges our knowledge of the big issue of Feshbach molecular formation.

In this paper, using a many-body two-channel microscopic Hamiltonian, we investigate the dynamics of Feshbach molecular formation in bosonic systems such as ^{85}Rb. We show that many-body effects alter the LZ picture of two-body molecular production through dramatically distorting the energy levels near the Feshbach resonance. With the help of a mean-field classical Hamiltonian, we derive an analytic expression for the conversion efficiency in the nonadiabatic regime. Our theory agrees with experimental data. Our theory thus is extended to the Feshbach formation of heteronuclear diatomic molecules such as ^{85}Rb-^{87}Rb and predicts that many-body effects are more significant there.

Our paper is organized as follows. In Sec. II, we present our model. In Sec. III, many-body effects on the conversion dynamics are addressed and an analytic expression for conversion efficiency is derived. In Sec. IV, we apply our theory to explain the experimental data. In Sec. V, we extend our theory to the heteronuclear molecules. The final section is our conclusion.

II. MODEL

Considering the experimental condition that the densities of the atom cloud is unusually low and the two- and three-body atomic decay and collisional molecular decay rates are negligible, we exploit the following two-channel model to describe the dynamics of converting atoms to molecules in the bosonic system,

$$\hat{H} = \epsilon_a \hat{a}^\dagger \hat{a} + \epsilon_b(t)\hat{b}^\dagger \hat{b} + \frac{g}{\sqrt{V}}(\hat{a}^\dagger \hat{a}^\dagger \hat{b} + \hat{b}^\dagger \hat{a}\hat{a}), \tag{1}$$

where $\hat{a}$ ($\hat{a}^\dagger$) and $\hat{b}(\hat{b}^\dagger)$ are Bose annihilation (creation) operators of atoms and molecules, respectively. $g = \sqrt{4\pi\hbar^2 a_{bg}\Delta B \mu_{co}/m}$ is the atom-molecule coupling due to the Feshbach resonance, m is the mass of a bosonic atom, a_{bg} is background scattering length, ΔB is the width of the resonance, and μ_{co} is the difference in the magnetic moment between the closed channel and open channel state. Here, we introduce parameter V to denote the volume of trapped particles and therefore $n=N/V$ is the mean density of initial bosonic atoms. The external magnetic field is linearly swept $B(t)=\dot{B}t$ and crosses the Feshbach resonance at B_0. The molecular energy under the field is $\epsilon_b(t)=\mu_{co}[B(t)-B_0]$. The total number of particles $N=\hat{a}^\dagger\hat{a}+2\hat{b}^\dagger\hat{b}$ is a conserved constant.

The above single-mode model is an approximate description of the clouds of noncondensed atoms and molecules,

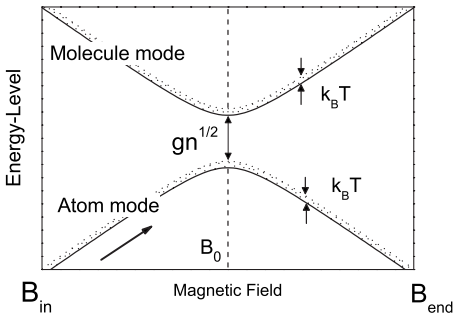

FIG. 1. Schematic plot of energy levels of atomic mode and molecular mode. Our single-mode approximation is valid only when the energy distribution of the thermal particles is much smaller than the effective width of the Feshbach resonance, i.e., $k_BT \ll \sqrt{g^2 n}$. Moreover, it is required that the time for the external magnetic field to sweep across the Feshbach resonance is smaller than the "dephasing" time $\tau_d = \frac{2\pi\hbar}{k_BT}$. For a detailed discussion refer to the text.

and is only valid when the energy distribution of the thermal particles (characterized by k_BT, k_B is the Boltzmann constant and T is the temperature) is much smaller than the effective Feshbach resonance width $g\sqrt{n}$. In such cases, each energy band of the thermal particles can be approximately denoted by one energy level, as schematically plotted in Fig. 1. Initially, the particles on one level have a definite phase and the phase difference between two levels is well defined. However, as the magnetic field sweeps across the Feshbach resonance from B_{in} to B_{end} at a rate of $\dot{B}$, particles will acquire additional phases that are proportional to their individual energy and sweeping time $(B_{\text{end}} - B_{\text{in}})/\dot{B}$. The varied particles in one level could acquire different phases because they have different energies. The validity of our single-mode approximation requires that the above mismatch in phase or dephasing is at least smaller than 2π, which defines a dephasing time $\tau_d = \frac{2\pi\hbar}{k_BT}$ [9]. When the time taken by the external magnetic field to sweep across the Feshbach resonance is smaller than the above dephasing time, i.e., $(B_{\text{end}} - B_{\text{in}})/\dot{B} < \frac{2\pi\hbar}{k_BT}$, the above dephasing effects can be ignored. The above analysis sets up a lower bound on the sweeping rate. So, in the following discussion, we focus on the fast-swept or nonadiabatic regime in which the above condition is satisfied.

Using the Fock states as a basis, the Schrödinger equation is written as

$$i\frac{d}{dt}|\psi\rangle = \hat{H}|\psi\rangle, \tag{2}$$

where $|\psi\rangle = \Sigma_{j=0}^{N/2} c_j |2j, N/2-j\rangle$, $|2j, N/2-j\rangle = \frac{1}{\sqrt{(2j)!(N/2-j)!}} \times (\hat{a}^\dagger \hat{a}^\dagger)^j (\hat{b}^\dagger)^{N/2-j} |0\rangle$ $(j=0,\ldots,N/2)$ are Fock states, and c_j is the probability amplitudes on the corresponding Fock state, respectively. The normalization condition is $\Sigma_j |c_j|^2 = 1$.

For the simplest case of $N=2$, the above Schrödinger equation reduces to the following two-level system of Landau-Zener type:

$$i\hbar\frac{d}{dt}\begin{pmatrix} c_0 \\ c_1 \end{pmatrix} = \begin{pmatrix} \epsilon_b & v/2 \\ v/2 & 2\epsilon_a \end{pmatrix}\begin{pmatrix} c_0 \\ c_1 \end{pmatrix}, \tag{3}$$

where $|c_0|^2$ and $|c_1|^2$ denote the population of molecules and atoms, respectively. For the two-level system, the energy bias between two levels is $\gamma = (2\epsilon_a - \epsilon_b)$ and the coupling strength is given by $v = 2g\sqrt{n}$. Initially, all particles populate in the lower level of the atomic state, i.e., $c_0 = 0, c_1 = 1$. When the external magnetic field is linearly swept across the Feshbach resonance at $\gamma \simeq 0$, a fraction of atoms will be converted to molecules at the avoided crossing of energy levels. The conversion efficiency as a function of the sweeping rate (i.e., $\dot{\gamma} = \mu_{co}\dot{B}$) and coupling strength takes the form [5]

$$\Gamma_{lz} = 1 - \exp\left(-\frac{\pi v^2}{2\hbar\dot{\gamma}}\right) = 1 - \exp\left(-\frac{8\pi^2 n\hbar|a_{bg}\Delta B|}{m|\dot{B}|}\right). \tag{4}$$

The above is the two-body molecular production picture and is consistent with the result from the coupled-channel scattering calculation in Ref. [7].

Mathematically, ignoring a total phase, the dynamics of Eq. (3) are equivalent to the following simple classical Hamiltonian [10,11]:

$$\mathcal{H}_{lz} = -\gamma/\hbar s + v/\hbar\sqrt{1-s^2}\cos\theta, \tag{5}$$

where the canonical conjugate variables are the population difference $s = |c_0|^2 - |c_1|^2$ and the relative phase $\theta = \arg c_0 - \arg c_1$. The dynamics are governed by the canonical equations of $\dot{\theta} = \frac{\partial\mathcal{H}_{lz}}{\partial s}$, $\dot{s} = -\frac{\partial\mathcal{H}_{lz}}{\partial\theta}$. The fixed points satisfying $\dot{s} = 0$, $\dot{\theta} = 0$ correspond to the extremum of system energy. These classical fixed points correspond to the eigenstates of quantum equations (3) and their energies (corresponding to the eigenvalues of quantum eigenstates) are calculated and plotted against the energy bias parameter γ in Fig. 2(a). It exhibits a typical LZ avoided-crossing configuration. Initially, all particles populate in the atomic state of $s_0 = -1$ at the left-hand end of the lower level. When the external field passes through the Feshbach resonance of width $v/\hbar$ at $\gamma = 0$, a fraction of atoms are converted to molecules at the right-hand end of the lower level, leading to a variation in the population variable, i.e.,

$$s_f = 2\Gamma_{lz} - 1 = 1 - 2\exp\left(-\frac{\pi v^2}{2\hbar\dot{\gamma}}\right). \tag{6}$$

As we go beyond the above two-body treatment to consider the many-body effects, the structure of the energy levels will change dramatically and the above LZ formula of the conversion efficiency will be altered due to many-body effects.

III. MANY-BODY EFFECTS IN FORMING HOMONUCLEAR FESHBACH MOLECULES

To include many-body effects, we need to solve full $\frac{N}{2}+1$ dimensional quantum equations (2). Using the basis of Fock states, the Schrödinger equation is rewritten as

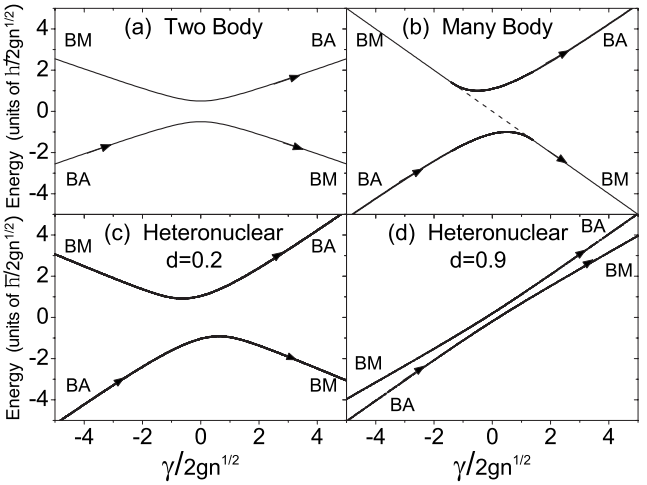

FIG. 2. Energy levels versus the scaled external magnetic fields. (a) Homonuclear two-body case; (b) homonuclear many-body case ($N=\infty$), where the dashed line represents an additional unstable eigenstate; (c),(d) heteronuclear many-body cases ($N=\infty$), where parameter d denotes initial population imbalance between two species.

$$i\frac{dc_j}{dt} = \sum_k H_{jk}c_k \quad (j,k=0,1,\ldots,N/2), \tag{7}$$

where the Hamiltonian matrix elements are $H_{jk}=\langle 2j,N/2-j|H|2k,N/2-k\rangle$. For $j=k$, $H_{jj}=j\gamma$; for $j\neq k$, $H_{jk}=0$ except $H_{j,j+1}=H_{j+1,j}=\sqrt{(j+1)(2j+1)(N/2-j)/2N}v$.

The above differential equations do not have explicit analytic solutions. We thus solve them numerically using the fourth- through fifth-order Runge-Kutta algorithm with an adaptive time step. Our result is presented in Fig. 3, which shows that the molecular conversion is altered due to many-body effects. Interestingly, there exists a crossing point between the two-body conversion curve and the many-body conversion curve. As the scaled inverse sweep rate is below this crossing point, the many-body effects enhance the molecular conversion efficiency, while as the scaled inverse sweep rate is above the crossing point, the many-body effects

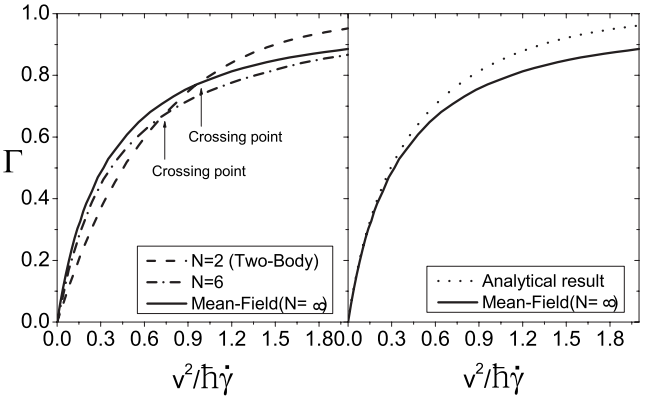

FIG. 3. Feshbach molecular production efficiency versus the scaled inverse sweep rates. As we increase the number N of the particles, the many-body result converges to the mean-field curve.

suppress the molecular conversion efficiency. The location of the crossing point is dependent on the total particle number N and shifts to the right as N increases. For $N=6$, the crossing point corresponds to $v^2/\hbar\dot{\gamma}=0.7$. It shifts to one as $N=\infty$.

Below, with the help of angular momentum operators, we deduce an analytic expression for the atom-molecule conversion efficiency under the mean-field approximation. The angular momentum operators are introduced as follows [12]:

$$\hat{L}_x = \sqrt{2}\frac{\hat{a}^\dagger\hat{a}^\dagger\hat{b}+\hat{b}^\dagger\hat{a}\hat{a}}{N^{3/2}}, \tag{8}$$

$$\hat{L}_y = \sqrt{2}i\frac{\hat{a}^\dagger\hat{a}^\dagger\hat{b}-\hat{b}^\dagger\hat{a}\hat{a}}{N^{3/2}}, \tag{9}$$

$$\hat{L}_z = \frac{2\hat{b}^\dagger\hat{b}-\hat{a}^\dagger\hat{a}}{N}. \tag{10}$$

The operator L_z denotes the atom-molecule population imbalance, and L_x, L_y describe the coherence of atoms and molecules. They compose a generalized Bloch representation [13]. The commutators between the operators are $[\hat{L}_z,\hat{L}_x]=\frac{4i}{N}\hat{L}_y$, and $[\hat{L}_z,\hat{L}_y]=-\frac{4i}{N}\hat{L}_x, [\hat{L}_x,\hat{L}_y]=\frac{i}{N}(1-\hat{L}_z)(1+3\hat{L}_z)+\frac{4i}{N^2}$. $\hat{L}_x,\hat{L}_y,\hat{L}_z$ do not span SU(2) because the commutator $[\hat{L}_x,\hat{L}_y]$ yields a quadratic polynomial in L_z. The generalized Bloch surface is determined by the conserved relationship $(\hat{L}_x)^2+(\hat{L}_y)^2=\frac{1}{2}(1+\hat{L}_z)(1-\hat{L}_z)^2+\frac{2}{N}(1-\hat{L}_z)+\frac{4}{N^2}\hat{L}_z$. The Hamiltonian (1) becomes $\hat{H}=-\frac{N}{4}\gamma\hat{L}_z+\frac{\sqrt{2}N}{4}v\hat{L}_x$ [14]. The Heisenberg equations are $i\hbar\frac{d}{dt}\hat{L}_j=[\hat{L}_j,\hat{H}]$, $j=x,y,z$.

In the mean-field limit where $N\to\infty$, all the above commutators vanish. Therefore, it is appropriate to replace L_x, L_y, and L_z by their expected values u, w, and s, respectively. Noting the constraint $u^2+w^2=\frac{1}{2}(s-1)^2(s+1)$ and introducing the conjugate angular variable $\theta=\arctan(w/u)$ denoting the relative phase between atoms and molecules, the Heisenberg equations can be replaced by a classical Hamiltonian of the form

$$\mathcal{H}_m = -\gamma/\hbar s + v/\hbar\sqrt{(1-s^2)(1-s)}\cos\theta. \tag{11}$$

To understand the dynamics, we first look at the fixed points $\dot{s}=\dot{\theta}=0$. The energies for these fixed points make up energy levels of the system, as shown in Fig. 2(b). The structure of these energy levels changes dramatically compared to the two-body case. We observe that (i) there are two fixed points when $|\gamma/v|$ is large enough: One for the bosonic molecule (BM) and the other for the bosonic atom (BA). (ii) When $|\gamma/v|<\sqrt{2}$, there is an additional fixed point with $s=1$. However, this fixed point is a saddle point corresponding to dynamically unstable quantum states [15]. Equation (11) and the energy spectra in Fig. 2(b) are the same as those obtained for the two-mode atom-molecule Fermi system [13,16] except that the sign of the magnetic field is reversed.

Compared to Hamiltonian (5), the coupling term in many-body Hamiltonian (11) is renormalized by a factor $\sqrt{1-s}$. So, the Feshbach resonance width that is proportional to the cou-

pling either broadens or shrinks depending on the factor. For the fast-sweep case, s should be not far from its initial value -1; therefore, the resonance width broadens and we expect that many-body effects enhance the atom-molecule conversion. In contrast, for the slow-sweep case, s may take a value close to 1; therefore, the resonance width shrinks. We then expect that the many-body effects suppress the atom-molecule conversion compared to the two-body Landau-Zener formula. The above analysis reveals the mechanism behind the crossing phenomenon exhibited in Fig. 3.

To derive an approximate analytic expression for the conversion efficiency, we introduce an effective coupling v_{eff} as

$$v_{\mathrm{eff}} = v\sqrt{1-s^*}, \tag{12}$$

where s^* can be approximately taken as the average between initial value $s_0=-1$ and the final value s_f, i.e., $s^*=(-1+s_f)/2$. Using the relation $\Gamma_m=2\langle\hat{b}^\dagger\hat{b}\rangle/N=(1+s_f)/2$ and formula (4), we obtain a self-consistent formula for the many-body conversion efficiency Γ_m,

$$\Gamma_m \simeq 1-\exp\left(-\frac{\pi v^2(2-\Gamma_m)}{2\hbar\dot{\gamma}}\right). \tag{13}$$

The above self-consistent equation for the conversion efficiency Γ_m can be readily solved using the iteration method. The result is presented in Fig. 3. We also numerically solve the mean-field equations using the Runge-Kutta step-adaptive algorithm. They are in good agreement, especially in the nonadiabatic regime of fast-sweep rates (see Fig. 3). For the slow-sweep case, the above formula overestimates molecular conversion slightly.

IV. COMPARISON WITH EXPERIMENT OF ^{85}Rb

Now we apply our theory to the ^{85}Rb experiment by the JILA group [8]. The atoms are held in a purely magnetic "baseball" trap. For efficient evaporation, the bias field is held at 162 G, where the scattering length is positive. For slow magnetic field ramps, Rb_2 molecules are produced only when the field is ramped upward through the resonance, which is located at 155 G. Hence, the first step in molecule production is to rapidly jump the magnetic field from 162 G to 147.5 G. They then sweep the field back up to 162 G at a chosen linear rate, producing molecules as they pass through the Feshbach resonance. The initial conditions of the atomic cloud are $N=87\,000$ and $n=1.3\times10^{11}$ cm^{-3}. The Feshbach resonance parameters are $a_{bg}=-443a_0$, $\Delta B=10.71$ G, and $\mu_{co}=-2.33\mu_B$, where a_0 and μ_B are the Bohr radius and Bohr magneton, respectively. The thermal cloud of the particles is at temperature $T=40$ nK.

In the first part of their experiment, they measured the molecular conversion efficiency as a function of the inverse ramp rate. A typical data set is shown in Fig. 4. The data are mainly divided into three regimes, i.e., the linear increase regime where the inverse ramp rates are less than 100 μs/G, the saturation regime where the inverse ramp rates are larger than 200 μs/G, and the transition regime in between. The single-mode approximation exploited in our theory requires that the resonance width is much larger than the energy distribution of the particles. In this experiment, we see that the ratio $g\sqrt{n}/k_BT$ is around 20 at $T=40$ nK. While in the saturation regime, the molecular conversion rates are found to saturate around 37%. From our "dephasing" criterion discussed in Sec. II, i.e., $(B_{\mathrm{end}}-B_{\mathrm{in}})/\dot{B}<\frac{2\pi\hbar}{k_BT}$ and that $B_{\mathrm{in}}=147.5$ G, $B_{\mathrm{end}}=162$ G, we have $1/\dot{B}<82$ μs/G. So, in our discussion, we only focus on the first regime. In Fig. 4, we plot the results from our many-body theory, which show good agreement with the experimental data in the linear regime. As a comparison, we also plot the result from the Landau-Zener formula, which shows a pronounced deviation from the experimental data.

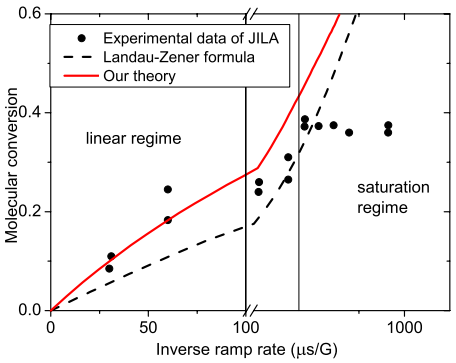

FIG. 4. (Color online) Molecular conversion efficiency versus the inverse sweeping rates.

In the second part of the experiment, to compare with Landau-Zener theory quantitatively, the JILA group measured the ratio between mean density and $1/e$ ramp rate as a function of mean density. They found that the Landau-Zener parameter predicted from the two-body theory is roughly 1/8 of the value extracted from the experimental data. They use the formula $N_{\mathrm{mol}}=N_{\mathrm{max}}(1-e^{-\alpha n\Delta B a_{bg}/\dot{B}})$ to fit the experimental data on molecular conversion, where N_{max} is the asymptotic number of molecules created for a very slow ramp, $\dot{B}$ is the magnetic field sweeping rate, and α is a fitting parameter. $\delta_{\mathrm{LZ}}=\alpha n\Delta B a_{bg}/\dot{B}$ is the Landau-Zener parameter. The saturation data in Fig. 4 indicate that $N_{\mathrm{max}}/N=37\%$. The $1/e$ ramp rate $\dot{B}_{1/e}$ is defined as that at $\dot{B}_{1/e}$, $\delta_{\mathrm{LZ}}=1$, and $N_{\mathrm{mol}}/N_{\mathrm{max}}=63\%$. It was then claimed that the data support a constant value for $n/\dot{B}_{1/e}$ (see Fig. 5). The value for α, extracted from the experimental data, is 4.5×10^{-7} m^2 s^{-1}. However, the two-body Landau-Zener formula (4) predicts $\alpha=8\pi^2\hbar/m=5.9\times10^{-8}$ m^2 s^{-1}, roughly 1/8 of the experimental data.

Now we apply our many-body theory to resolve this puzzle. At $B_{1/e}$, the molecular conversion efficiency is $N_{\mathrm{mol}}/N=37\%\times63\%=23\%$. In the nonadiabatic regime, our many-body formula (13) is simplified as $\Gamma_m\simeq\frac{16\pi^2n\hbar|a_{bg}\Delta B|}{m|\dot{B}|}$. Substituting $\Gamma_m=23\%$, $B=B_{1/e}$ into the above formula, we have $n/\dot{B}_{1/e}=\frac{0.23m}{16\pi^2\hbar|a_{bg}\Delta B|}=105\times10^{11}$ cm^{-3} μs G^{-1}, which is in good agreement with the experimental data of the fourth scatter in Fig. 5.

To compare with two-body LZ formula (4), we see that, the many-body effects change the $1/e$ rate in the nonadiabatic regime by a factor of 2. The above analysis uncovers

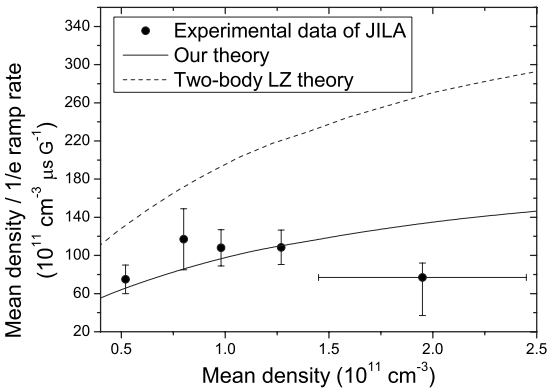

FIG. 5. The ratios of mean density over $1/e$ ramp rate, with respect to mean density. Our theory shows a good agreement with the experiment for four low density points but is obviously larger than the final point. At the high density, the cloud experienced significant heating during the ramps across the resonance, hence the density of the final point has significant uncertainty [8].

the physics behind the 1/8 deviation. The factor 1/8 is the product of the following three factors: 0.37 is from the maximum conversion rate, 0.63 is from the definition of the $1/e$ ramp rate, and 1/2 comes from many-body effects.

Our calculations are extended to the cases of varied spatial densities. As mentioned above, in Ref. [8], the formula $N_{\mathrm{mol}}=N_{\max}(1-e^{-\alpha n\Delta B a_{bg}/\dot{B}})$ is used to fit experimental data on molecular conversion. Accordingly, the $1/e$ ramp rate $B_{1/e}$ corresponds to $N_{\mathrm{mol}}/N_{\max}=1-1/e=63\%$. Our many-body theory equation (13) predicts that $n/\dot{B}_{1/e}=\frac{0.63m}{16\pi^2\hbar|a_{bg}\Delta B|}\frac{N_{\max}}{N}$. Because the maximum molecular conversion efficiency (i.e., $N_{\max}/N$) is a function of peak phase space density as revealed in Fig. 2 of Ref. [8] and the spatial density is proportional to peak phase space density at the fixed temperature, we claim that $n/\dot{B}_{1/e}$ is spatial density n dependent through $N_{\max}/N$. The $N_{\max}/N$ as a function of density is from Fig. 2 of Ref. [8]. Thus, our theoretical curve is plotted against the experimental data in Fig. 5. It shows good agreement with the experiment for four low density points but is obviously larger than the final point. At high density, the cloud experienced significant heating during the ramps across the resonance, hence the density of the final point has significant uncertainty (i.e., see the caption of Fig. 1 of [8]). The result from two-body LZ theory is also presented in Fig. 5 for comparison. It is 2 times as large as that of many-body theory, and obviously deviates from the experimental data.

V. MANY-BODY EFFECTS IN FORMING HETERONUCLEAR FESHBACH MOLECULES

In the above discussion, we investigated the dynamics of Feshbach converting single atomic species to homonuclear diatomic molecules. Actually, the Feshbach resonance technique has been used to produce heteronuclear molecules from two or more species of atoms [17]. These ultracold heteronuclear molecules in low-lying vibrational states are of particular interest since they could be a permanent dipole moment due to the unequal distribution of electrons. Other proposals for using the polar molecules include quantum computation [18] and testing fundamental symmetry [19].

In this section, we extend our discussion to the two-species atom case and show that the heteronuclear molecular production efficiency is more significantly altered due to many-body effects. The many-body three-channel Hamiltonian for the heteronuclear system reads as [20]

$$\hat{H}=\epsilon_{a1}\hat{a}_1^\dagger\hat{a}_1+\epsilon_{a2}\hat{a}_2^\dagger\hat{a}_2+\epsilon_b(t)\hat{b}^\dagger\hat{b}+\frac{g}{\sqrt{V}}(\hat{a}_1^\dagger\hat{a}_2^\dagger\hat{b}+\hat{b}^\dagger\hat{a}_1\hat{a}_2), \tag{14}$$

where $\hat{a}_1$ ($\hat{a}_1^\dagger$), $\hat{a}_2$ ($\hat{a}_2^\dagger$) are annihilation (creation) operators of the heteronuclear atoms and $\hat{b}$ ($\hat{b}^\dagger$) are annihilation (creation) operators of molecules, $g=\sqrt{2\pi\hbar^2 a_{bg}\Delta B\mu_{co}/m'}$ is the atom-molecule coupling strength, and $m'=m_1m_2/(m_1+m_2)$ is the reduced mass of two-atom scattering. The total number of particles $N=N_{a1}+N_{a2}+N_b=\hat{a}_1^\dagger\hat{a}_1+\hat{a}_2^\dagger\hat{a}_2+2\hat{b}^\dagger\hat{b}$ is a conserved constant. The density $n=N/V$.

Using the Fock states as a basis, the Schrödinger equation is written as

$$i\frac{d}{dt}|\psi\rangle=\hat{H}|\psi\rangle, \tag{15}$$

where $|\psi\rangle=\Sigma_{j=0}^{N/2}c_j|j,j,N/2-j\rangle$, $|j,j,N/2-j\rangle=\frac{1}{\sqrt{j!j!(N/2-j)!}}\times(\hat{a}_1^\dagger\hat{a}_2^\dagger)^j(\hat{b}^\dagger)^{N/2-j}|0\rangle$ $(j=0,\ldots,N/2)$ are Fock states, and c_j is the probability amplitude on the corresponding Fock state, respectively. The normalization condition is that $\Sigma_j|c_j|^2=1$.

For $N=2$, the Schrödinger equation reduces to

$$i\hbar\frac{d}{dt}\begin{pmatrix}c_0\\c_1\end{pmatrix}=\begin{pmatrix}\epsilon_b & v/2\sqrt{2}\\ v/2\sqrt{2} & \epsilon_{a1}+\epsilon_{a2}\end{pmatrix}\begin{pmatrix}c_0\\c_1\end{pmatrix}, \tag{16}$$

where $|c_0|^2$ and $|c_1|^2$ denote the population of molecules and atoms, respectively. The energy bias $\gamma=\epsilon_{a1}+\epsilon_{a2}-\epsilon_b$. Then, two-body molecular production efficiency is $1-\exp(-\frac{\pi v^2}{4\hbar\dot{\gamma}})$. Comparing the above expression with Eq. (4), a 1/2 factor emerges in the exponent. This is due to the distinguishability between two atomic species that decreases the effective density of each atomic species.

For the two-species case, the number of particles in each species may not be identical. Therefore, we introduce a parameter d to denote the population imbalance between the two species, i.e., $d\equiv(N_{a1}-N_{a2})/N$ assuming that $N_{a1}>N_{a2}$. Our concern is the conversion efficiency of type-2 atoms, i.e., $\Gamma_d=2N_b/(1-d)N$ when the magnetic field is swept across the resonance. We will show that d is an important parameter in forming the heteronuclear molecule. For the larger population imbalance, the heteronuclear molecule production is more significantly altered due to the many-body effect.

For the heteronuclear system, the Bloch space is expanded by the following three operators: $\hat{L}_x=2\sqrt{2}\frac{\hat{a}_1^\dagger\hat{a}_2^\dagger\hat{b}+\hat{b}^\dagger\hat{a}_1\hat{a}_2}{N^{3/2}}$, $\hat{L}_y=2\sqrt{2}i\frac{\hat{a}_1^\dagger\hat{a}_2^\dagger\hat{b}-\hat{b}^\dagger\hat{a}_1\hat{a}_2}{N^{3/2}}$, and $\hat{L}_z=\frac{2\hat{b}^\dagger\hat{b}-\hat{a}_1^\dagger\hat{a}_1-\hat{a}_2^\dagger\hat{a}_2}{N}$. The commutators between the operators are

$$[\hat{L}_z,\hat{L}_x]=\frac{4i}{N}\hat{L}_y, \tag{17}$$

$$[\hat{L}_z,\hat{L}_y] = -\frac{4i}{N}\hat{L}_x, \tag{18}$$

$$[\hat{L}_x,\hat{L}_y] = \frac{i}{N}[(1-\hat{L}_z)(1+3\hat{L}_z)+4d^2] + \frac{4i}{N^2}(1+\hat{L}_z). \tag{19}$$

The generalized Bloch surface is determined by the conserved relationship

$$(\hat{L}_x)^2 + (\hat{L}_y)^2 = \left(1+\hat{L}_z+\frac{4}{N}\right)[(1-\hat{L}_z)^2+4d^2]. \tag{20}$$

Hamiltonian (14) becomes $\hat{H}=-\frac{N}{4}\gamma\hat{L}_z+\frac{N}{4\sqrt{2}}v\hat{L}_x$. The Heisenberg equations are $i\hbar\frac{d}{dt}\hat{L}_j=[\hat{L}_j,\hat{H}]$, $j=x,y,z$. In the mean-field limit where $N\to\infty$, it is appropriate to replace L_x, L_y, and L_z by their expected values u, w, and s, respectively. Noting the constraint $u^2+w^2=(1+s)[(1-s)^2-4d^2]$ and introducing the conjugate angular variable $\theta=\arctan(w/u)$ denoting the relative phase between atoms and molecules, the Heisenberg equations can be replaced by a classical Hamiltonian of the form

$$\mathcal{H}_m^d = -\frac{\gamma}{\hbar}s + \frac{v}{\sqrt{2}\hbar}\sqrt{(1+s)[(1-s)^2-4d^2]}\cos\theta, \tag{21}$$

and the canonical equations,

$$d\theta/dt = -\frac{\gamma}{\hbar} - \frac{v}{2\sqrt{2}\hbar}\frac{(1-s)(1+3s)+4d^2}{\sqrt{(1+s)[(1-s)^2-4d^2]}}\cos\theta, \tag{22}$$

$$ds/dt = \frac{v}{\sqrt{2}\hbar}\sqrt{(1+s)[(1-s)^2-4d^2]}\sin(\theta). \tag{23}$$

The fixed points of the above system have been obtained by setting $\dot{s}=\dot{\theta}=0$. The energies for these fixed points make up energy levels of the system, as shown in Figs. 2(c) and 2(d). The structure of these energy levels changes dramatically compared to the homonuclear case. There are always two fixed points corresponding to two branches of energy levels. Moreover, for a large population imbalance between two species, for example, $d=0.9$, the energy levels tend to parallel each other [see Fig. 2(d)]. Thus, the level space remains almost constant and is slightly dependent on the external field. We therefore expect that molecular efficiency is very large in this case.

Compared to Hamiltonian (5), the coupling term in many-body Hamiltonian (21) is renormalized by a factor of $\sqrt{\frac{(1-s)^2-4d^2}{2(1-s)}}$. To derive an approximate expression, we use the effective coupling v_{eff} as $v_{\text{eff}}=v\sqrt{\frac{(1-s^*)^2-4d^2}{2(1-s^*)}}$, where s^* can be approximately taken as the average between the initial value $s_0=-1$ and the final value s_f, i.e., $s^*=(-1+s_f)/2$. Using the relation $\Gamma_d=2N_b/N(1-d)=(1+s_f)/2(1-d)$ and formula (6), we obtain a self-consistent formula for the many-body conversion efficiency Γ_d,

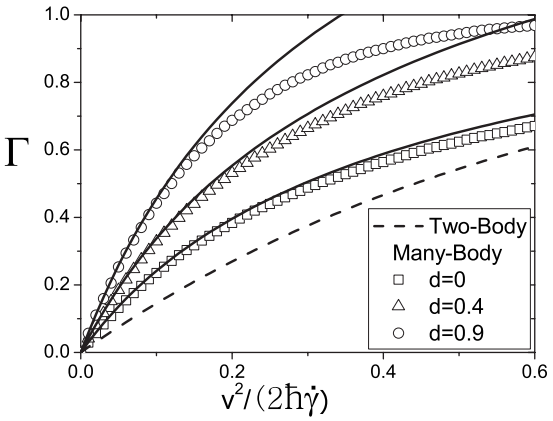

FIG. 6. Feshbach heteronuclear molecule production efficiency versus the scaled inverse sweep rate. The solid curves are our analytical result. For details refer to the text.

$$(1-d)\Gamma_d \simeq 1-\exp\left(-\frac{\pi v^2[2(1-d^2)-\Gamma_d(1-d)(1+d^2)]}{4\hbar\dot{\gamma}}\right). \tag{24}$$

The above self-consistent equation for the conversion efficiency Γ_d can be readily solved using the iteration method. The result is presented in Fig. 6. We also numerically solve the mean-field equations for comparison using the Runge-Kutta step-adaptive algorithm. The agreement is good in the nonadiabatic regime where the conversion rate is less than 0.6 (see Fig. 6). For $d=0.9$, the regime corresponds to an inverse scaled sweep rate less than 0.15. It extends to $v^2/2\hbar\dot{\gamma}<0.6$ for $d=0$. Increasing the population imbalance parameter d means that the effective density of type-2 atoms decreases, but at the same time a type-2 atom has more chance to collide with its partner, the type-1 atom, because the density of type-1 atoms increases. The competition between these two effects leads to an enhancement of heteronuclear molecular conversion efficiency in the nonadiabatic regime. Outside the nonadiabatic regime, our analytic formula overestimates the production efficiency. This deviation is mainly due to the difference in the range of s of Hamiltonian (5) and (21), respectively, i.e., it is $[-1,1-2d]$ in the heteronuclear case and $[-1,1]$ in the homonuclear case. This complicates the slowly sweeping case when we use Eq. (6) as the starting point of our iteration scheme.

In the nonadiabatic regime, the conversion efficiency of the heteronuclear molecule can be approximated to $\Gamma_d \simeq \frac{(1+d)8\pi^2\hbar|a_{bg}\Delta B|n}{m\dot{B}}$. Defining the $1/e$ ramp rate $\dot{B}_{1/e}$ as that at $\dot{B}_{1/e}$, $\Gamma_d=1/e$, then, the ratio $n/\dot{B}_{1/e}=\frac{m}{(1+d)8e\pi^2\hbar|a_{bg}\Delta B|}$ is predicted to be independent of the density but inversely proportional to the imbalance parameter.

Experimentally, our theory may apply to the ^{85}Rb-^{87}Rb system. In Ref. [17], the heteronuclear molecules of ^{85}Rb-^{87}Rb have been produced using the Feshbach resonance technique, where one BEC and a thermal gas of the second species are used. The main experimental parameters are $a_{bg}=240a_0$, $\Delta B=4.9$ G, $n=1\times10^{14}$ cm^{-3}. We then can calculate that the dimensionless inverse sweeping rate $v^2/(2\hbar\dot{\gamma})$

$=0.57$ corresponds to the real sweep rate of a practical magnetic field $\dot{B}=0.1$ G/μs. However, to apply our theory, we suggest that the experiment should be performed under low atom cloud densities such as $n\sim 10^{11}$ cm^{-3} with both species prepared as thermal gas of a few tens of nK.

VI. CONCLUSION

In conclusion, we have investigated the dynamics of the Feshbach formation of the molecules in bosonic systems and shown that the many-body effects greatly modify the picture of two-body molecular production. With the help of a mean-field classical Hamiltonian, we derive an analytic expression for the conversion efficiency and explain the discrepancy between the prediction of the Landau-Zener formula and the experimental data on ^{85}Rb. Our theory solves a puzzle on the formation of Feshbach molecules and gives some predictions on the formation of heteronuclear diatomic molecules such as ^{85}Rb-^{87}Rb.

ACKNOWLEDGMENTS

This work is supported by the National Natural Science Foundation of China (Contracts No. 10725521 and No. 10604009) and the National Fundamental Research Programme of China under Grants No. 2006CB921400 and No. 2007CB814800.

[1] J. J. Hudson, B. E. Sauer, M. R. Tarbutt, and E. A. Hinds, Phys. Rev. Lett. **89**, 023003 (2002).
[2] C. A. Regal, M. Greiner, and D. S. Jin, Phys. Rev. Lett. **92**, 040403 (2004).
[3] E. Timmermans, P. Tommasini, M. Hussein, and A. Kerman, Phys. Rep. **315**, 199 (1999).
[4] T. Köhler, K. Góral, and P. S. Julienne, Rev. Mod. Phys. **78**, 1311 (2006).
[5] L. D. Landau, Phys. Z. Sowjetunion **2**, 46 (1932); G. Zener, Proc. R. Soc. London, Ser. A **137**, 696 (1932).
[6] F. H. Mies, E. Tiesinga, and P. S. Julienne, Phys. Rev. A **61**, 022721 (2000).
[7] K. Goral, T. Koehler, S. A. Gardiner, E. Tiesinga, and P. S. Julienne, J. Phys. B **37**, 3457 (2004).
[8] E. Hodby, S. T. Thompson, C. A. Regal, M. Greiner, A. C. Wilson, D. S. Jin, E. A. Cornell, and C. E. Wieman, Phys. Rev. Lett. **94**, 120402 (2005).
[9] See, for example, E. Eisenberg, K. Held, and B. L. Altshuler, Phys. Rev. Lett. **88**, 136801 (2002).
[10] J. Liu, L. Fu, B. Ou, S. Chen, D. Choi, B. Wu, and Q. Niu, Phys. Rev. A **66**, 023404 (2002).
[11] J. Liu, B. Wu, and Q. Niu, Phys. Rev. Lett. **90**, 170404 (2003).
[12] A. Vardi, V. A. Yurovsky, and J. R. Anglin, Phys. Rev. A **64**, 063611 (2001).
[13] E. Pazy, I. Tikhonenkov, Y. B. Band, M. Fleischhauer, and A. Vardi, Phys. Rev. Lett. **95**, 170403 (2005); I. Tikhonenkov, E. Pazy, Y. B. Band, M. Fleischhauer, and A. Vardi, Phys. Rev. A **73**, 043605 (2006).
[14] This Hamiltonian is exactly the one obtained for fermionic systems in [13] if we reverse the sign of operator $\hat{L}_z$. In [13], it was assumed that the number of the available fermionic states equals the total number of particles. Validity of this assumption was commented by D. Sun, A. Abanov, and V. L. Pokrovsky, e-print arXiv:0707.3630. Nevertheless, in the deduction of the Hamiltonian for our bosonic system, this assumption is not required. As will be shown later, a "renormalized" Landau-Zener formula derived from the Hamiltonian is able to account for the experimental findings in the nonadiabatic regime.
[15] J. R. Anglin, Phys. Rev. A **67**, 051601(R) (2003); J. Liu, C. Zhang, M. G. Raizen, and Q. Niu, *ibid.* **73**, 013601 (2006); G.-F. Wang, D.-F. Ye, L.-B. Fu, X.-Z. Chen, and J. Liu, *ibid.* **74**, 033414 (2006).
[16] Jie Liu, Li-Bin Fu, Bin Liu, and Biao Wu, e-print arXiv:0704.3867.
[17] S. B. Papp and C. E. Wieman, Phys. Rev. Lett. **97**, 180404 (2006).
[18] A. Micheli, G. K. Brennen, and P. Zoller, Nat. Phys. **2**, 341 (2006).
[19] M. G. Kozlov and L. N. Labzowsky, J. Phys. B **28**, 1933 (1995).
[20] L. Zhou, W. Zhang, H. Y. Ling, L. Jiang, and H. Pu, Phys. Rev. A **75**, 043603 (2007).